Geophys. J. Int. (1997) **130,** 193–200

A three-dimensional spherical mesh generator

M. E. Everett

Department of Geology and Geophysics, Texas A&M University, College Station TX 77843, *USA*

Accepted 1997 March 12. Received 1997 February 25 ; in original form 1996 September 25

SUMMARY

A new spherical mesh generator is described. It represents an efficient, deterministic packing of tetrahedra into a solid sphere, a spherical shell, or both. The mesh can be used for finite-element solutions to a wide variety of global numerical modelling problems in the geosciences. The nodes within the mesh are distributed uniformly, and long, thin tetrahedra are avoided. The method proposed here offers several advantages over 3-D Delaunay algorithms for finite-element mesh generation. For the related problem of trivariate scattered data interpolation, which is not considered here, the 3-D Delaunay algorithms are the method of choice.

Key words: finite-element methods.

INTRODUCTION

Many global numerical modelling problems in the geosciences involve solving systems of differential equations over a spherical domain, or within a thick spherical shell. Examples include atmospheric (e.g. Wyman 1996) and oceanographic (e.g. Semtner & Chervin 1988) general circulation, buoyancy-driven flow for geoid prediction (e.g. Zhang & Christenson 1993), mantle convection (e.g. Bercovici 1995), seismic wave propagation (e.g. Cummins, Geller & Takeuchi 1994), core dynamo evolution (e.g. Glatzmaier & Roberts 1995), and electromagnetic induction (e.g. Everett & Schultz 1996). The governing sets of equations for the spatially dependent variables are generally solved by spectral, finite-difference (FD) or hybrid spectral–FD methods. Less frequently, they are solved by the finite-element (FE) method. The FE method offers many advantages over the prevailing methods, but suffers from the perception that problems are difficult to formulate and algorithms difficult to implement.

In this contribution, a new 3-D spherical mesh generator is introduced. It is useful for problems where a tetrahedral decomposition of a thick spherical shell, or the entire solid sphere, is appropriate, such as in finite-element methods. The development of the new mesh generator was motivated by the success of a finite-element model of electromagnetic induction in the spherical earth (Everett & Schultz 1996). The purpose of this paper is to demonstrate that a simple, high-quality tetrahedralization of the sphere, or a thick spherical shell, is straightforward to attain. It is hoped that this demonstration will stimulate a more widespread investigation into the use of finite-element and related methods for other global modelling problems, such as those listed above. A large body of previous work has been concerned with 2-D spherical triangulations covering the surface of a sphere (e.g. Cullen 1974; Baumgardner & Frederickson 1985; Augenbaum & Peskin 1985; Constable, Parker & Stark 1993; Wang & Dahlen 1995) but little has been published on solid 3-D spherical tetrahedralizations.

The mesh described here has two principal advantages over its predecessor in Everett & Schultz (1996): (1) the radial node density is very small at the centre of the sphere, increases exponentially to some arbitrary radius (which may be inside, outside, or on the surface of the sphere), and then remains constant to some arbitrary outer radius; (2) all tetrahedra are well-shaped, i.e. there are no long, thin ones. The mesh retains the desired property that the angular distribution of nodes in the polar and azimuthal coordinates is very uniform. In addition, the north and south poles do not require any special consideration, as they do for curvilinear grids oriented along lines of constant latitude and longitude. Furthermore, the mesh generation is not based on triangulating a randomly generated set of points in 3-D space. In short, the new mesh is an efficient, deterministic packing of tetrahedra into a sphere.

SPHERICAL MESH GENERATION

In recent years several strategies have developed for 3-D tetrahedral meshing of arbitrarily shaped bodies: recursive spatial decompositions or octrees (Shephard & Georges 1991); 3-D Delaunay triangulations (Yuen, Tan & Hung 1991; Sambridge, Braun & McQueen 1995); advancing-front methods (Peraire *et al.* 1988); and convex polyhedral decomposition (Joe 1994). Our strategy for tetrahedralizing the solid sphere, or a thick spherical shell, is most similar to the convex decomposition technique.

The mesh is a composite of two parts: an interior part, and an exterior part. The two parts are seamlessly welded together by a common polyhedral surface. The interior mesh is a tetrahedralization of the solid sphere. Its radial node density increases exponentially with radius. The exterior mesh is a tetrahedralization of a thick spherical shell. The radial node density is constant with radius. Depending on the application,

© 1997 RAS

Downloaded from https://academic.oup.com/gji/article-abstract/130/1/193/865040 by Texas A&M University user on 21 September 2018

the exterior or the interior mesh can be used alone, or the full composite mesh can be used.

The interior mesh

The approach for constructing the interior mesh is recursively to subdivide an initial polyhedral decomposition of the sphere consisting of seven vertices (nodes) and eight tetrahedra. This decomposition is referred to as refinement level 0 (Fig. 1, top left) and consists of a node at the centre of the sphere, a node at each pole, and equatorial nodes on the 0°, 90°, 180°, and 270° meridians. The nodes are triangulated by eight identical tetrahedra: four in the northern hemisphere and four in the southern hemisphere tetrahedra, as shown in the figure.

Each of the tetrahedra in refinement level 0 is further refined into eight subtetrahedra (Fig. 2) according to the method of Liu & Joe (1996). In this method, each triangular facet of the tetrahedron is refined into four subtriangles by connecting new nodes placed at the midpoints of the six edges. This yields four new subtetrahedra at the corners of the original tetrahedron, plus an octohedron in the middle (Fig. 2, top right). The central octohedron is then decomposed into an additional four subtetrahedra by adding an interior edge. This can be done in three different ways (Fig. 2, bottom). The interior edge chosen is the one that maximizes the sum of the quality factors (see below) of the four new subtetrahedra that are created.

The integrity of a tetrahedron is measured here by its quality factor, Q. Poorly shaped tetrahedra are to be avoided wherever possible, since they can adversely affect the performance of a numerical method. Liu & Joe (1996) define the quality factor of a tetrahedron as

$$Q = 12(3V)^{3/2} \sum_{i \neq j} L_{ij}^2, \tag{1}$$

where V is the volume of the tetrahedron and L_{ij} is the length

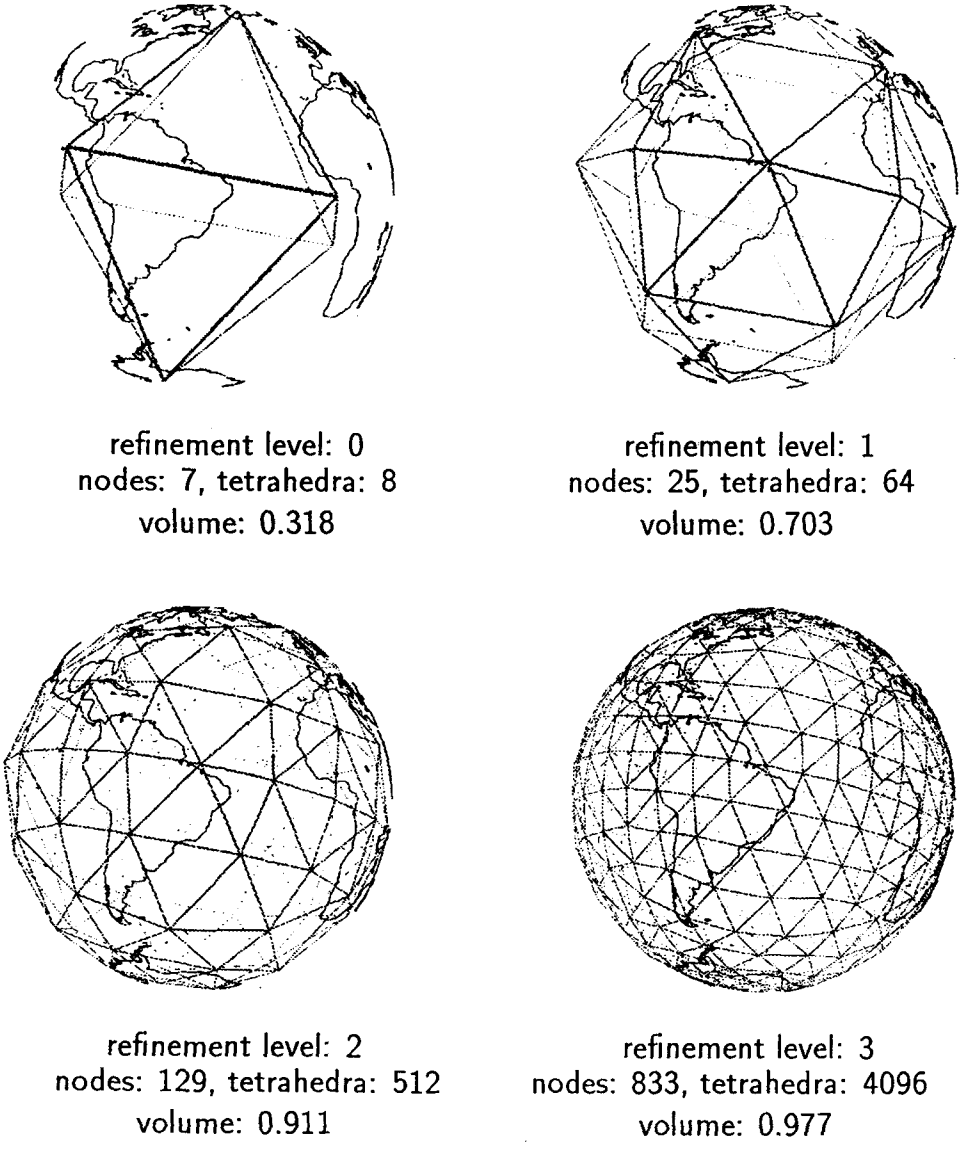

Figure 1. Successive refinements of the initial polyhedral approximation of the solid sphere. The number of nodes and tetrahedra are indicated for each refinement, as well as the volume occupied as a fraction of the volume of the sphere. Not all the nodes are shown in the diagrams; for example in refinement level 0 there is a hidden node at the centre of the sphere. The varying line weight from solid to faintly dashed is intended as depth cueing.

Downloaded from https://academic.oup.com/gji/article-abstract/130/1/193/865040 by Texas A&M University user on 21 September 2018

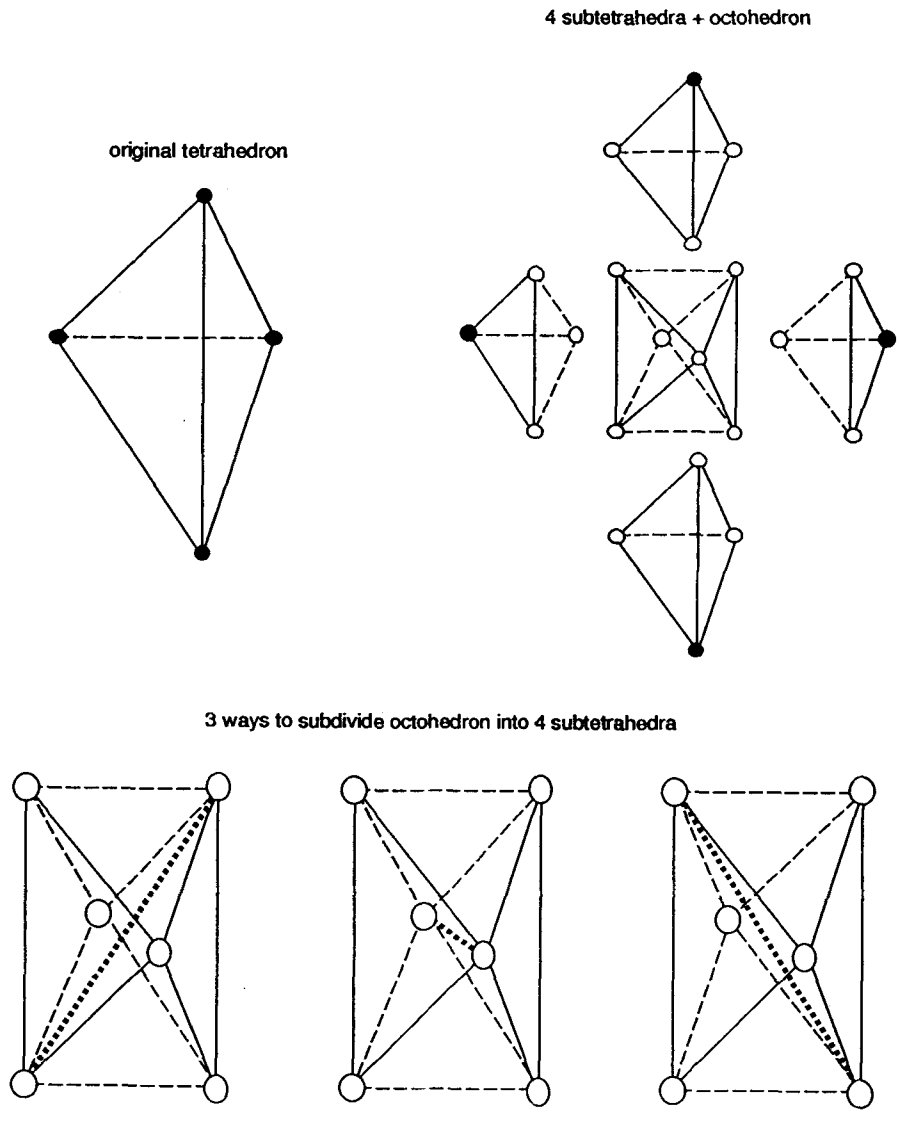

Figure 2. Subdivision of a tetrahedron into eight subtetrahedra.

of the edge joining vertex i and vertex j. The quality factor Q varies between 0 and 1. The lower limit corresponds to poorly shaped tetrahedra, while the upper limit corresponds to well-shaped, or regular tetrahedra. Quality factors are shown in Fig. 3 for a sequence of tetrahedra generated by continuously varying the position of a vertex along a straight line.

Successive refinements of the initial polyhedral approximation to the sphere are shown in the remainder of Fig. 1. For example, the refinement at some level i is generated by a subdivision of each tetrahedron belonging to refinement level $i-1$ into eight subtetrahedra, as described above. There is one additional complication that must be taken into account. During the refinement process, as shown in Fig. 2, new nodes are added to the midpoints of edges of triangular facets. However, certain tetrahedra contain facets whose three vertices are coincident with the surface of the sphere. The radii of the newly added midpoint nodes for these facets are less than the radius of the sphere, since the nodes are added midway along the chord between vertices. To ensure that successive refinements of the tetrahedral mesh conform as closely as possible to the curved geometry of the sphere, the positions of the newly added nodes must be projected outwards from the interior onto the surface of the sphere along a line emanating from the origin. This procedure, along with the analogous procedure in two dimensions for triangulating a disc, is illustrated in Fig. 4.

The distributions of several mesh quality diagnostics for the interior mesh at refinement level 4 (6071 nodes, 32 768 tetrahedra) are shown in Fig. 5. This refinement level occupies a fraction 0.994 of the volume of the unit sphere. The quality factors range from 0.6 to 1.0, with the distribution peaking at $Q > 0.9$, indicating a very high-quality mesh. The radial distribution of nodes follows an approximate exponential distribution, from near zero at the origin to a maximum at the outer radius. This form of radial distribution is appropriate for two reasons: (1) the volume occupied by a spherical shell of a given radial thickness τ falls off as the cubed power of the shell's average radius; and (2) for many solid-sphere applications, high accuracy is demanded near the surface where observations are made. The polar distribution of nodes is maximum at the equator ($\cos\theta = 0$) and falls off symmetrically with increasing latitude to near zero at the poles ($\cos\theta = \pm 1$).

Downloaded from https://academic.oup.com/gji/article-abstract/130/1/193/865040 by Texas A&M University user on 21 September 2018

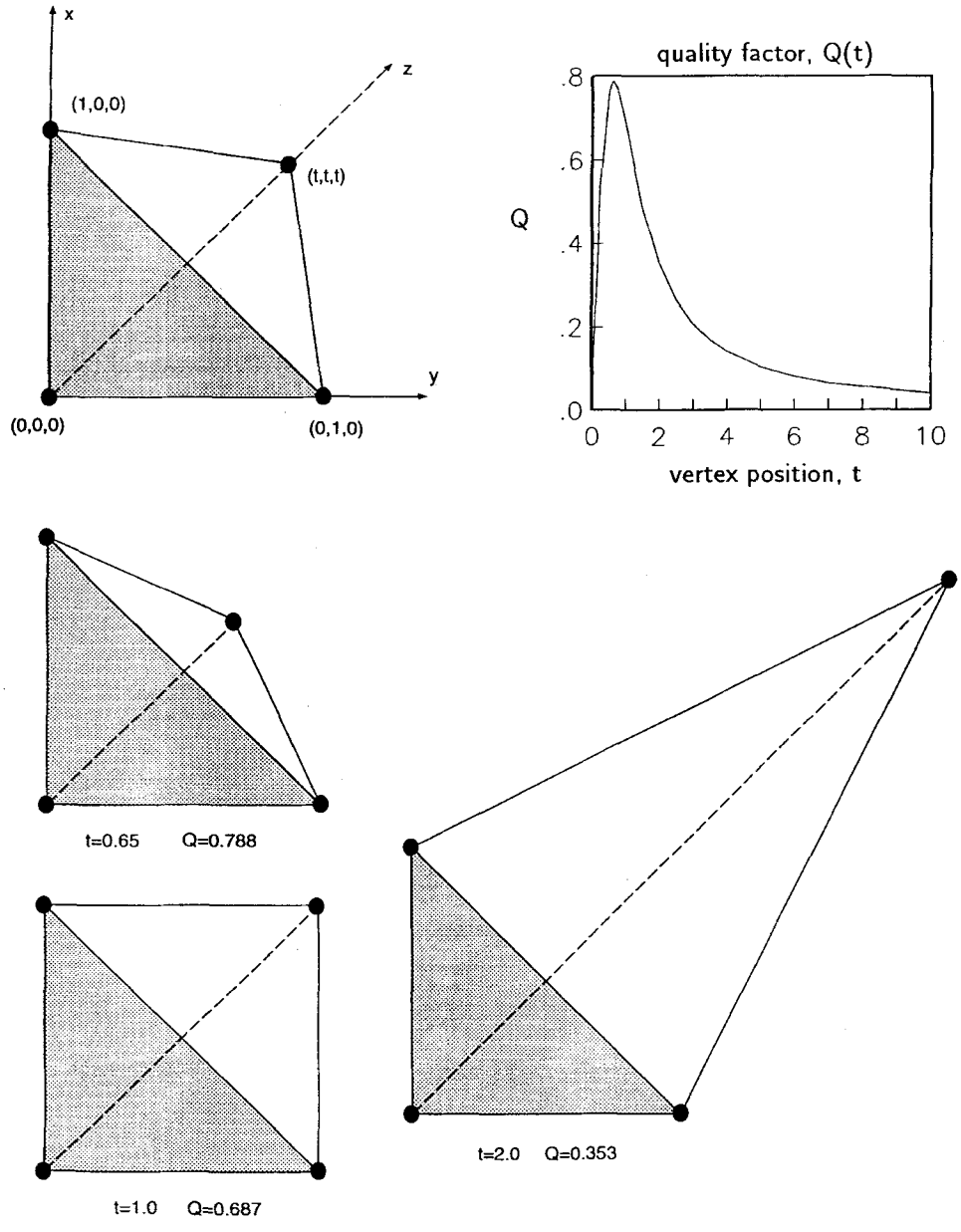

Figure 3. Quality factor as a function of tetrahedron shape. The vertex coordinates are as marked. The parameter t is varied between 0.0 and 10.0. Changing the parameter t changes the shape, and hence the quality factor, of the tetrahedron. Several representative examples are shown.

The azimuthal distribution is uniform, except at the meridians, $\phi = 0°$, 90°, 180°, 270°, where a higher-than-average node density is noted. This is a reflection of the placement of the initial set of nodes in refinement level 0 (see Fig. 1).

The exterior mesh

A tetrahedralization of the solid sphere is appropriate for finite-element solutions to problems in seismic wave propagation or core dynamo evolution where the Earth's inner core is part of the solution domain. However, in problems such as ocean and atmospheric general circulation and mantle convection, tetrahedralizing a spherical shell is more efficient, since the inner regions of the Earth need not be part of the solution domain. Furthermore, for some problems, such as global electromagnetic induction where the solutions in the air and the Earth must both be calculated but have different characteristic spatial wavelengths, a composite mesh is required consisting of tetrahedralizations of both an exterior spherical shell and interior solid sphere.

The construction of the exterior (spherical shell) mesh begins by considering the triangulation on the outer surface of the interior mesh. A portion of this triangulation is shown in Fig. 6. A new triangulation is created by projecting the nodes and edges radially outwards along lines emanating from the origin of the sphere. New edges are created to connect the two triangulations, as shown in the figure. An arbitrary number of these triangulations can be so connected, nested together at different characteristic radii. All that remains to complete the construction of the exterior mesh is to tetrahedralize the basic solid-geometric unit, termed a 'barrel triangular prism', shown at the bottom in Fig. 6.

Downloaded from https://academic.oup.com/gji/article-abstract/130/1/193/865040 by Texas A&M University user on 21 September 2018

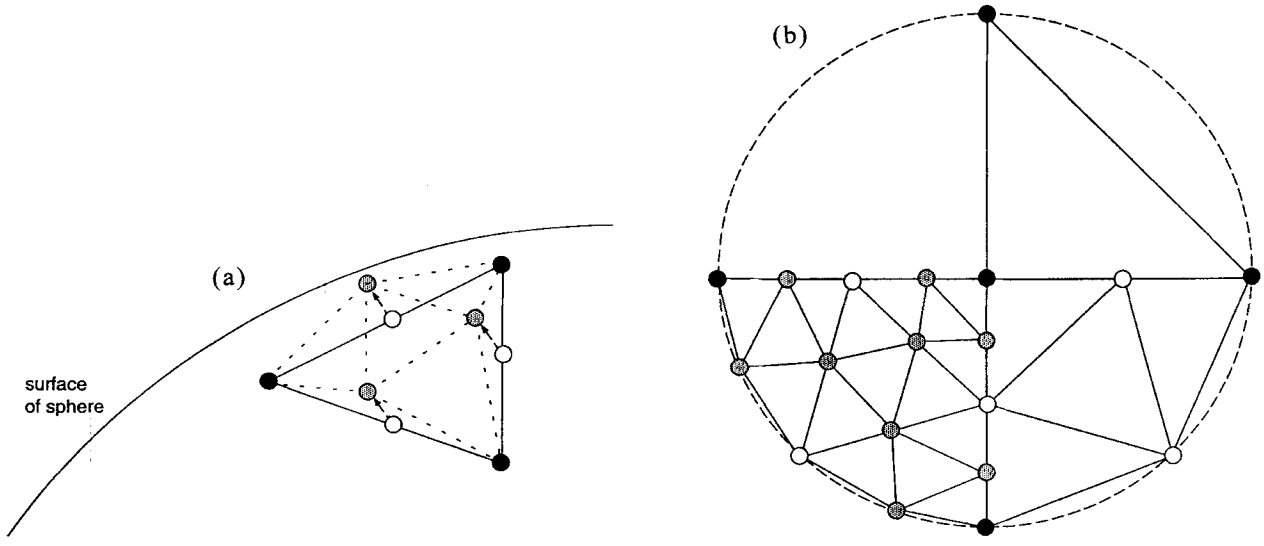

Figure 4. (a) Procedure for projecting newly added nodes to the surface of the sphere. The dark circles are vertices of the original triangulation, and they lie on the surface of the sphere. The open circles are newly added nodes, which lie on chords between the dark circles and hence are beneath the surface of the sphere. The shaded circles are the newly added nodes projected onto the surface of the sphere along a line emanating from the origin. The dotted lines show the refined triangulation. (b) The analogous procedure in two dimensions for triangulating the disc. A coarse initial triangulation is indicated in the top, right quadrant of the disc. The first refinement is shown in the bottom, right quadrant. A second refinement is shown in the bottom, left quadrant. During each refinement, the newly added nodes (open circles in the first refinement; shaded circles in the second refinement) on the surface of the disc were projected there from their initial positions on chords connecting pre-existing surface nodes.

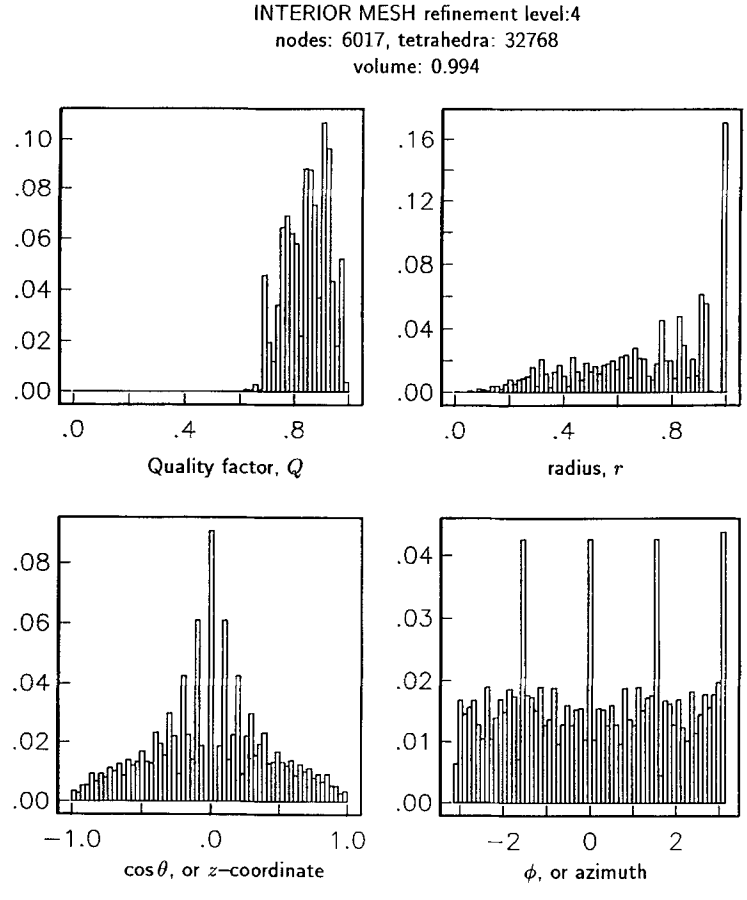

Figure 5. Frequency histograms showing interior-mesh quality factors and spatial distributions of nodes.

Downloaded from https://academic.oup.com/gji/article-abstract/130/1/193/865040 by Texas A&M University user on 21 September 2018

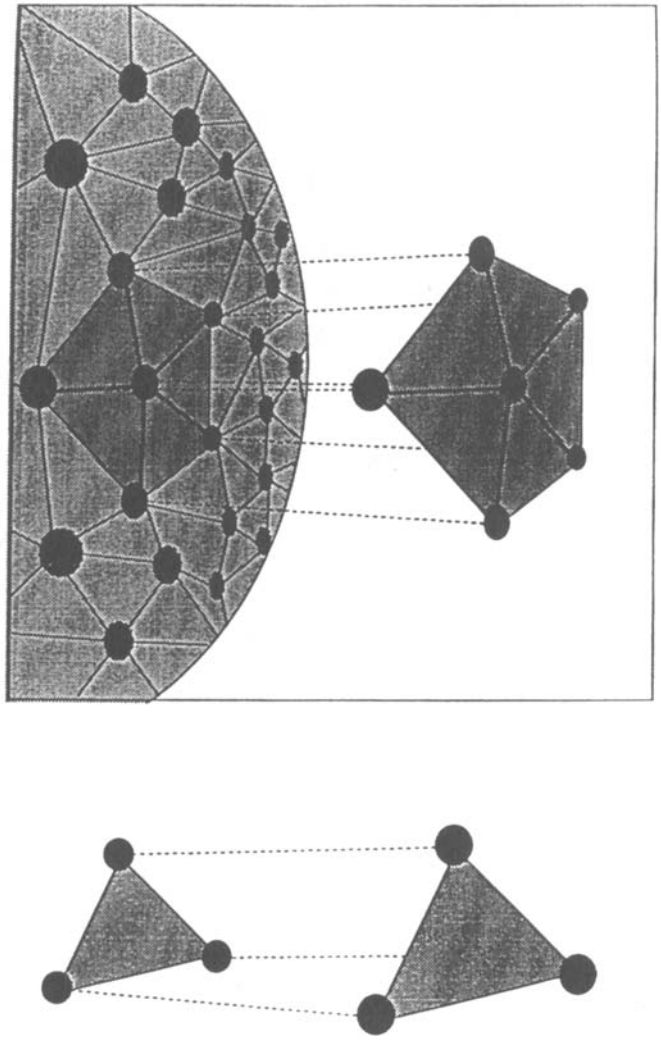

Figure 6. Construction of the exterior mesh. See text for details.

The barrel triangular prism is readily decomposed into three subtetrahedra. A particular decomposition is shown in Fig. 7. The distributions of several mesh quality diagnostics for the exterior mesh at refinement level 3 (1548 nodes, 9216 tetrahedra) are shown in Fig. 8. The quality factors range from 0.65 to 0.9, with the distribution peaking at Q slightly less than 0.8, again indicating a very high-quality mesh. The radial distribution of nodes is a series of identical delta functions. The positions of the delta functions correspond to the characteristic radii of the nested spherical triangulations. In the example shown, six triangulations were nested with geometrically increasing characteristic radii, the largest of which was equal to four times the radius of the interior mesh. The geometric spacing factor between adjacent triangulations is 1.3. The polar and azimuthal distributions of nodes in the exterior mesh (not shown) are identical to those of the interior mesh.

DISCUSSION

The spherical mesh generator described in this paper can be used to solve problems in the geosciences which involve solving partial differential equations in a spherical, or spherical-shell, domain. The lack of a good mesh generator may be one contributing factor to the slow development of finite-element methods in 3-D global numerical modelling. It is hoped that this paper will contribute to a re-examination of FE methods for this purpose, with the eventual goal of improving accuracy, efficiency and providing alternative solutions to validate the existing spectral/FD techniques.

The mesh generator described in this paper is intended to serve as a front-end to a 3-D partial differential equation solver in spherical geometry. It is not intended to function as the framework for trivariate interpolation of scattered data within a sphere. This important problem has been addressed by numerous authors, including Sambridge *et al.* (1995), who considered 2-D and 3-D Delaunay triangulations of *a priori* defined sets of points. The Delaunay algorithms are well-suited for scattered data interpolation, but in my experience they are

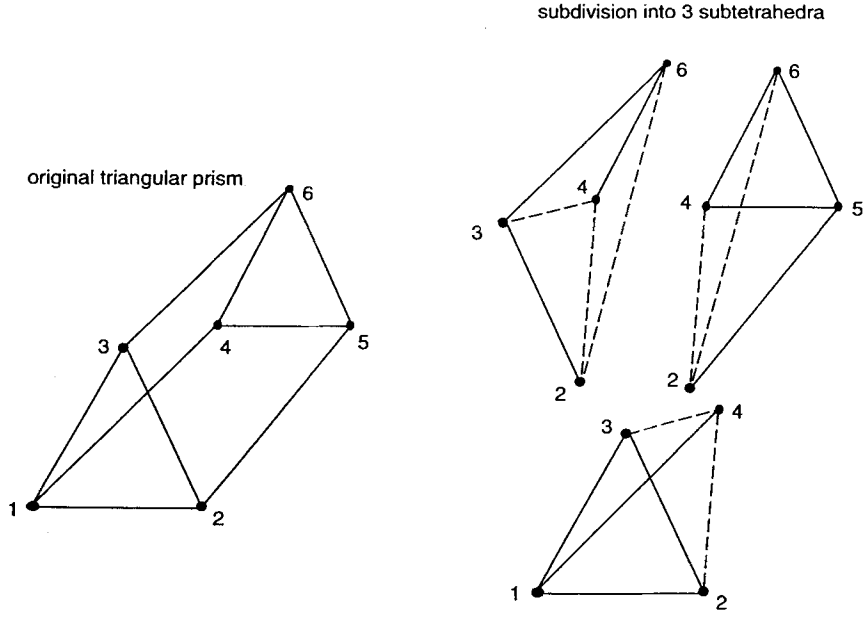

Figure 7. Subdivision of a barrel triangular prism into three subtetrahedra.

Downloaded from https://academic.oup.com/gji/article-abstract/130/1/193/865040 by Texas A&M University user on 21 September 2018

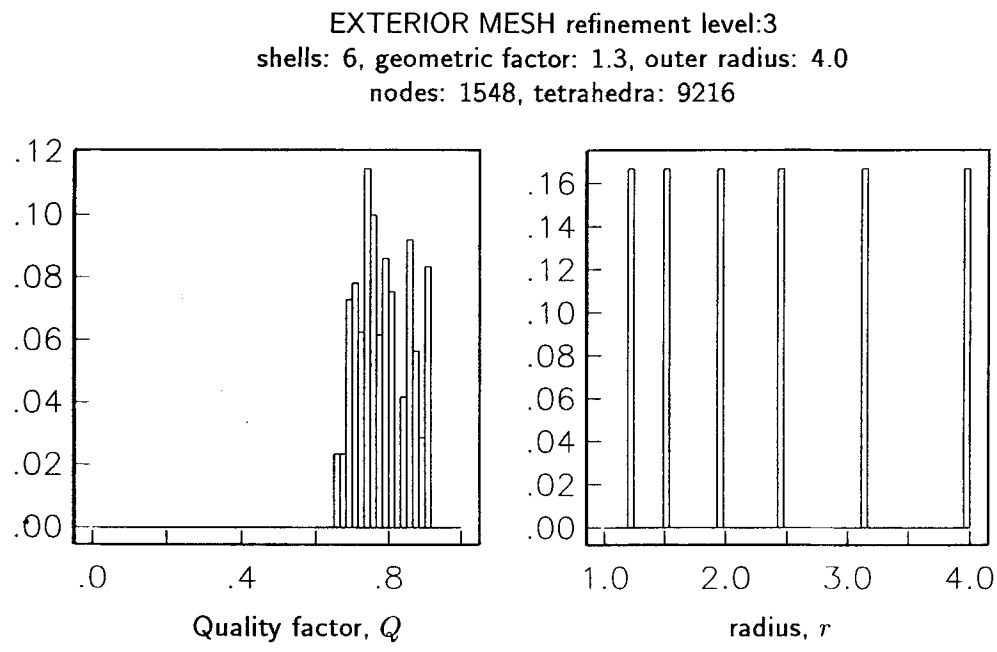

Figure 8. Frequency histograms showing exterior-mesh quality factors and radial distribution of nodes.

less well-suited for finite-element mesh generation. The reasons are twofold: (1) The Delaunay approach provides an optimal triangulation of arbitrarily placed points, but the triangulation is only as good as the point-set from which it is derived. How does one generate an optimal 3-D point-set from which to triangulate? For example, what if the *a priori* points span only a portion of the entire solid sphere? This would be the case in modelling just a single subduction zone, for example. How is the remainder of the sphere to be filled with points? In short, the Delaunay approach to mesh generation requires that a good, front-end point-set generator is available. (2) The Delaunay triangulation unavoidably produces long, thin tetrahedra if the *a priori* point-set is irregularly distributed. The occurrence of long, thin tetrahedra in a finite-element mesh degrades the conditioning of the finite-element matrix and slows or prevents the convergence of iterative solutions. The approach I recommend is to solve the partial differential equations on a high-quality, regular mesh (giving a stable matrix inversion) and then interpolate the resulting solution onto irregularly spaced points where the solution is required. A high-quality local mesh-refinement algorithm (e.g. Liu & Joe 1996, see below) should be used if a more detailed mesh in certain regions is deemed necessary.

The mesh developed here does not suffer from the 'pole problem' which plagues FD grids, whose cells oriented along constant longitudes converge at the pole. Furthermore, the tetrahedralization of the sphere, or spherical shell, lends itself readily to parametrizing Earth structure in terms of locally defined basis functions, such as trivariate spherical splines (Weiss & Everett 1996; see also Wang & Dahlen 1995 for bivariate spherical splines defined on the surface) or natural neighbour interpolants (Sambridge *et al.* 1995). Some of the spectral techniques for global modelling parametrize the Earth in terms of basis functions with global support, such as spherical harmonics. Global bases are not well-suited for accurate representations of regional variations superimposed on a relatively uniform background model (e.g. Weiss & Everett 1996).

Finally, local refinement of the basis-function support is often a difficult option when using spectral or FD techniques. The tetrahedralization described here is straightforward to refine locally (Liu & Joe 1996) and work is presently underway. For example, if Earth structure underneath, say, Japan is particularly interesting, one can refine just those tetrahedra that intersect the sub-Japanese region of interest, and leave the rest alone. The paper by Liu & Joe (1996) gives a recipe for performing a high-Q local mesh refinement. Their algorithm is elegant and does not leave extra nodes at the edges of refined tetrahedra.

ACKNOWLEDGMENTS

I would like to thank Adam Schultz, Jan Garmany, Chet Weiss, Heiner Igel and Malcolm Sambridge for very stimulating discussions on this topic. The mesh generator software is available on request from the author by e-mail at colt45@beerfrdg.tamu.edu.

REFERENCES

Augenbaum, J.M. & Peskin, C.S., 1985. On the construction of the Voronoi mesh on a sphere, *J. comput. Phys.*, **59**, 177–192.

Baumgardner, R.B. & Frederickson, P.O., 1985. Icosahedral discretization of the two-sphere, *SIAM J. numer. Anal.*, **22**, 1107–1115.

Bercovici, D., 1995. A source–sink model of the generation of plate tectonics from non-Newtonian mantle flow, *J. geophys. Res.*, **100**, 2013–2030.

Constable, C.G., Parker, R.L. & Stark, P.B., 1993. Geomagnetic field models incorporating frozen-flux constraints, *Geophys. J. Int.*, **113**, 419–433.

Downloaded from https://academic.oup.com/gji/article-abstract/130/1/193/865040 by Texas A&M University user on 21 September 2018

Cullen, M.J.P., 1974. Integrations of the primitive equations on a sphere using the finite element method, *Quart. J. R. meteor. Soc.*, **100,** 555–562.

Cummins, P.R., Geller, R.J. & Takeuchi, N., 1994. DSM complete synthetic seismograms: P–SV, spherically symmetric, case, *Geophys. Res. Lett.*, **21,** 1663–1666.

Everett, M.E. & Schultz, A., 1996. Geomagnetic induction in a heterogeneous sphere: azimuthally symmetric test computations and the response of an undulating 660-km discontinuity, *J. geophys. Res.*, **101,** 2765–2783.

Glatzmaier, G.A. & Roberts, P.H., 1995. A three-dimensional convective dynamo solution with rotating and finitely conducting inner core and mantle, *Phys. Earth planet. Inter.*, **91,** 63–75.

Joe, B., 1994. Tetrahedral mesh generation in polyhedral regions based on convex polyhedron decompositions, *Int. J. num. Meth. Eng.*, **37,** 693–713.

Liu, A. & Joe, B., 1996. Quality local refinement of tetrahedral meshes based on 8-subtetrahedron subdivision, *Math. Comp.*, **215,** 1183–1200.

Peraire, J., Peiro, J., Formaggia, L., Morgan, K. & Zienkiewicz, O.C., 1988. Finite element Euler computations in three dimensions, *Int. J. num. Meth. Eng.*, **26,** 2135–2159.

Sambridge, M., Braun, J. & McQueen, H., 1995. Geophysical parametrization and interpolation of irregular data using natural neighbours, *Geophys. J. Int.*, **122,** 837–857.

Semtner, A.J. & Chervin, R.M., 1988. A simulation of the global ocean circulation with resolved eddies, *J. geophys. Res.*, **93,** 15 502–15 552.

Shephard, M.S. & Georges, M.K., 1991. Automatic three-dimensional mesh generation by the finite octree technique, *Int. J. num. Meth. Eng.*, **32,** 709–749.

Wang, Z. & Dahlen, F.A., 1995. Spherical-spline parameterization of three-dimensional Earth models, *Geophys. Res. Lett.*, **22,** 3099–3102.

Weiss, C.J. & Everett, M.E., 1996. Alternative parameterization of Earth models: 3-D spherical splines (abstract), *13th Workshop on Electromagnetic Induction in the Earth Onuma, Japan*, p. 75.

Wyman, B.L., 1996. A step-mountain coordinate general circulation model: description and validation of medium-range forecasts, *Mon. Wea. Rev.*, **124,** 102–121.

Yuen, M.M.F., Tan, S.T. & Hung, K.Y., 1991. A hierarchial approach to automatic finite element mesh generation, *Int. J. num. Meth. Eng.*, **32,** 501–525.

Zhang, S. & Christensen, U., 1993. Some effects of lateral viscosity variations on geoid and surface velocities induced by density anomalies in the mantle, *Geophys. J. Int.*, **114,** 531–547.

Downloaded from https://academic.oup.com/gji/article-abstract/130/1/193/865040 by Texas A&M University user on 21 September 2018